

PAPER

The effects of ICP dry etching and HF wet etching on the morphology of SiO₂ surface

To cite this article: Kazy F Shariar *et al* 2018 *Mater. Res. Express* **5** 095903

View the [article online](#) for updates and enhancements.

Related content

- [Technical Note](#)

Kyu-Youn Hwang, Chin-Sung Park, Joon-Ho Kim *et al.*

- [Surface modification of](#)

[poly\(dimethylsiloxane\) through oxygen and nitrogen plasma treatment to improve its characteristics towards biomedical applications](#)

N Gomathi, I Mishra, S Varma *et al.*

- [Surface energy-tunable iso decyl acrylate based molds for low pressure-nanoimprint lithography](#)

Hyowon Tak, Dongha Tahk, Chanho Jeong *et al.*



IOP | ebooksTM

Bringing you innovative digital publishing with leading voices to create your essential collection of books in STEM research.

Start exploring the collection - download the first chapter of every title for free.

Materials Research Express



PAPER

RECEIVED
11 May 2018

REVISED
15 July 2018

ACCEPTED FOR PUBLICATION
24 July 2018

PUBLISHED
8 August 2018

The effects of ICP dry etching and HF wet etching on the morphology of SiO₂ surface

Kazy F Shariar¹ , Jie Zhang¹, Keith Coasey², Md Abu Sufian¹, Roddell Remy², Jing Qu², Michael Mackay² and Yuping Zeng¹

¹ Department of Electrical and Computer Engineering, University of Delaware, Newark, DE-19711, United States of America

² Department of Material Science and Engineering, University of Delaware, Newark, DE-19711, United States of America

E-mail: yzeng@udel.edu

Keywords: surface morphology, dry and wet etching, surface adhesion, contact angle

Abstract

Both dry etching and wet etching are an integral part for the fabrication of semiconductor devices. However, both types of etching can cause problems such as surface degradation, uncontrollability of etching depth and undercut. For instance, aqueous HF (wet etching) and dry etching are used to etch SiO₂ films. During HF partial etch (SiO₂ is not fully removed), it introduces some interesting phenomena such as adhesion degradation on SiO₂ surface morphology which is not present when SiO₂ is fully etched. This paper reports the first study of systematical characterization of the SiO₂ surface morphology after partial dry and HF wet etching and compares their different effects on the strength of adhesion on polaric and nonpolar liquids. To study the strength of adhesion, this experiment utilized two different types of resist such as PMMA resist and PMGI based LOR resist. Atomic Force Microscopy (AFM) was used to determine the surface morphology before and after dry etching and HF wet etching process. Telescope-Goniometer was used to measure the contact angles as an indicator of liquid-solid adhesion. From the comparison study it's evident that partial wet etching by HF changes the surface morphology of the SiO₂ significantly and degrades the adhesion between the resist and the surface. On the other hand, dry etching does not alter the SiO₂ surface morphology significantly and it is recommended to use dry etching instead of HF wet etching to avoid the degradation in adhesion strength on SiO₂ surface whenever possible. Next, as a more general approach, adhesion promoter was used to restore the adhesion between the resist and SiO₂ surface.

1. Introduction

Nanodevice fabrication processing consists of methods such as dry and wet etching, metal deposition, sputtering, patterning etc. These fabrication methods interact with the surface of the substrate differently and change the surface characteristics. Some fabrication processes like hydrofluoric acid (HF) wet etching which is used extensively to etch SiO₂ alters the surface morphologies drastically and introduces resist adhesion-related problems.

The strength of adhesion of the resist patterns has been recognized as a serious problem during the fabrication process and has been studied extensively [1, 2]. Adhesion of resist to the surface of the substrate depends on several factors such as the chemistry of the resist [3], surface tension and wetting of materials and adhesion [2], substrate surface chemistry and condition [4]. One of the earliest efforts to understand the mechanism of resist pattern collapse was studied by Toshihiko Tanaka *et al* [5]. They correlated resist pattern collapse with the critical aspect ratio and surface tension of the rinsing liquid and proposed a low surface tension rinse process. J Bauer *et al* [2] discussed the surface tension and adhesion of different resist on Si and SiO₂ using contact angle. Their study proposed that pretreatment of the substrate such as cleaning, dehydration and exposure to humidity influences the surface tension. They also found that modifications by primers (hexamethyldisilazane and trimethylsilyldiethylamine) help to stabilize the surface tension. S K Kim *et al* [1] later

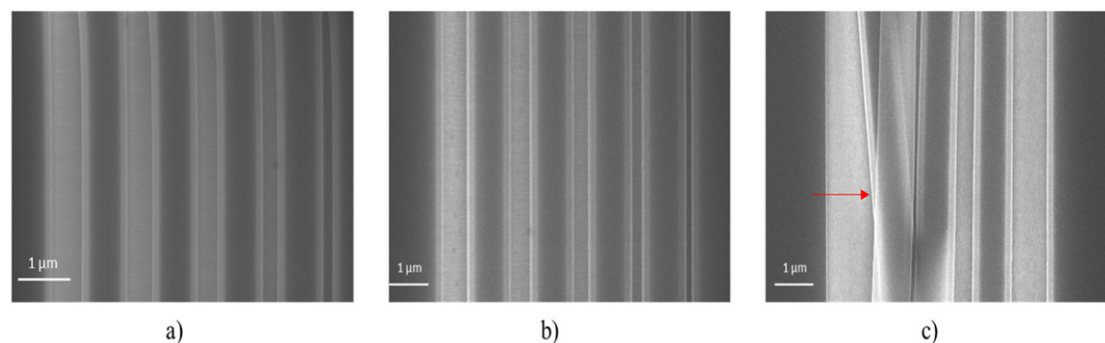


Figure 1. SEM image of written pattern on SiO_2/Si surface with PMGI based LOR resist (a) without any etching after e-beam exposure and development (sample A); (b) patterns after dry etching (sample B); (c) patterns after HF wet etching (sample C).

developed a process to measure the collapsing force of the photoresist patterns using an atomic force microscope (AFM). Additionally, they employed the lateral force microscope (LFM) to determine the load and moment of pattern collapse.

Another aspect of our study is to investigate the change in surface morphology after HF wet etching and its effect on surface adhesion. The etching process of SiO_2 by HF molecules has been studied extensively in previous literature [6–8]. T Hoshino *et al* [6] studied the mechanism of the etching reaction of silicon dioxide (SiO_2) by HF molecules and their reaction paths. T Takahagi *et al* [7] developed a procedure to clean the silicon surface with HF and ultraviolet (UV) cleaning. Most of this literatures discuss the chemistry of the SiO_2 etching rather the surface morphology of the SiO_2 surface after etching. Although J Bauer *et al* [2] discussed the surface tension and adhesion of different resist on Si and SiO_2 using contact angle; change of surface morphology after HF wet etching and its effect was not discussed.

All of the above-mentioned factors lead to the lithographic pattern error. A common patterning error is the collapse of the structure which can occur via three main pathways; bending, breaking and peeling from the surface. While the bending and breaking of the resist are related to its hardness, peeling is closely related to adhesion to the underlying layer [1]. Tremendous research work has been done to explore the breaking and bending of the collapsed resists which occurs during the development and/or rinsing process of photoresist [5, 9–12]. These types of collapse mainly originate from a capillary force [5]. The surface tension of the developer liquid between the resist structures causes the collapse of the structures [9]. Although many authors have made efforts to explain the photoresist bending and breaking phenomena [10–12], little literature was found focusing on peeling of the photoresist [13, 14]. A Kawai *et al* [13] characterized the resist pattern adhesion and cohesion in deionized water using direct peeling with an atomic microscope (AFM) tip (DPAT) method. They proposed that in DI water liquid intrusion acts to weaken the adhesion strength between resist and substrate.

In this study, we observed the LOR(PMGI) resist stack peeling off after wet etching of SiO_2 . To study the exact nature of surface properties changes, we investigated samples with different surface treatments. The patterns employed in this study are of a relatively low aspect ratio. We found that samples without any treatment do not show any adhesion problem. However, samples subjected to HF wet treatment show surface adhesion problem. As the patterns are low aspect ratio, the main mechanism of structural failure is caused by peeling off from the substrate surface rather than breaking or bending.

2. Experimental details

The e-beam written patterns with PMGI based LOR resist and PMMA resist on SiO_2/Si surface are shown in figures 1 and 2, respectively. The line widths are 500 nm, 400 nm, 300 nm, 200 nm and 100 nm respectively with a spacing of 1 micron. This experiment used Czochralski (CZ) Silicon wafers (Silicon Valley Microelectronics) with $\langle 100 \rangle$ orientation as the substrate. The SiO_2 layer thickness was 260 nm before any process was applied. Small ($10 \text{ mm} \times 10 \text{ mm}$) wafer pieces were used in the experiment. Three categories of samples were prepared for this experiment. Sample 'A' was the control sample without any treatment. Sample 'B' underwent Inductively Coupled Plasma (ICP) dry etching for 45 s in a Cl_2/Ar (5:15 ratio) atmosphere. The ICP and RF power were 100 W and 65 W, respectively. Samples 'C' were dipped into diluted HF (HF:DI = 2:98) for 120 s. After that E-beam lithography samples were prepared using spin coating. Bilayer resist was then applied for e-beam patterning. For PMGI based LOR resist, the first layer was LOR (PMGI Microchem) which was spun at 6000 rpm for 60 s, followed by baking at 170°C for 5 min. A layer of CSAR (AR-P 6200 Allresist) was then spun on top of the LOR film at a speed of 4000 rpm for 60 s then baked at 200°C for 5 min. For PMMA samples, the

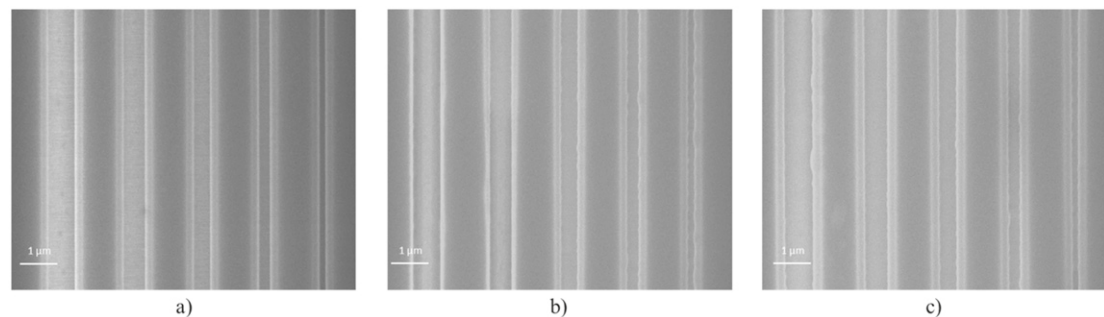


Figure 2. SEM image of written pattern on SiO_2/Si surface with PMMA resist (a) without any etching after e-beam exposure and development (sample A); (b) patterns after dry etching (sample B); (c) patterns after HF wet etching (sample C).

first layer was EL6 which was spun cast at 4000 rpm for 60 s followed by baking at 170°C for 5 min. A layer of PMMA 950 A2 was then spun on top of the EL6 film at a speed of 4000 rpm for 60 s then baked at 170°C for 5 min. E-beam lithography (Vistec EBPG5200ES) was used to write the patterns on the samples. $200 \mu\text{C cm}^{-2}$ base dose was used for PMGI based LOR resist and $600 \mu\text{C cm}^{-2}$ base dose was used for PMMA and EL6 resist.

Figure 1 shows the samples written with PMGI based LOR resist. Figure 1(a) shows the designed pattern written on the SiO_2 surface without any treatment or etching (sample A). Figure 1(b) shows the same pattern written on ICP dry etched (partially) SiO_2 surface (sample B). The SEM images show partial dry etching does not affect the surface and the resist adhesion problem is not visible. Figure 1(c) shows the same pattern written on HF treated samples (sample C). The SEM images show how the resist patterns dislodged from the substrate and overlapped with each other compared to the designed patterns of figure 1(a). From the SEM images it is evident that the resist is peeling off from the surface indicating a significant reduction in the adhesive force between the resist and the surface.

Figure 2 shows the samples written with PMMA and EL6 resist. Figures 2(a)–(c) shows no significant changes in the surface adhesion. This indicates that adhesion of resist to the surface is dependent not only on surface morphology but also on the chemical properties of resist as well. Following sections of this paper will investigate both parameters and discuss how the combination of surface morphology and resist chemistry leads to peeling off effect on partially HF wet etched SiO_2 surface.

Figure 3(a) shows an optical microscope image of sample C after e-beam exposure and development. Wavy patterns are obvious from the picture. Due to the discoloration at both ends of the resist line structure, it was initially thought that the undercut of the resist was much wider than expected. However, figures 3(c) and (d) shows that the undercut of the resist is minimal and as wide as expected. Figure 3(b) again confirms the surface adhesion problem between the resist and HF treated SiO_2 surface.

3. Surface characterization using AFM

To examine how the dry etching process and HF treatment change the properties of the SiO_2 surface, samples were examined using AFM.

3.1. Surface roughness characterization

The surface roughness can be characterized using centerline Roughness Average (R_a) and Root Mean Square (RMS) Roughness. R_a is the arithmetic average of the absolute values of the roughness profile ordinates given by equation (1). The average roughness is the area between the roughness profile and its mean line, or the integral of the absolute value of the roughness profile height over the evaluation length. The Root Mean Square (RMS), R_q , average between the height deviations and the mean line/surface, taken over the evaluation length/area.

$$R_a = \frac{1}{n} \sum_{i=1}^n |Z_i| \quad (1)$$

$$R_q = \sqrt{\frac{1}{n} \sum_{i=1}^n Z_i^2} \quad (2)$$

where Z_i is the amplitude of the point i and n is the number of sample points.

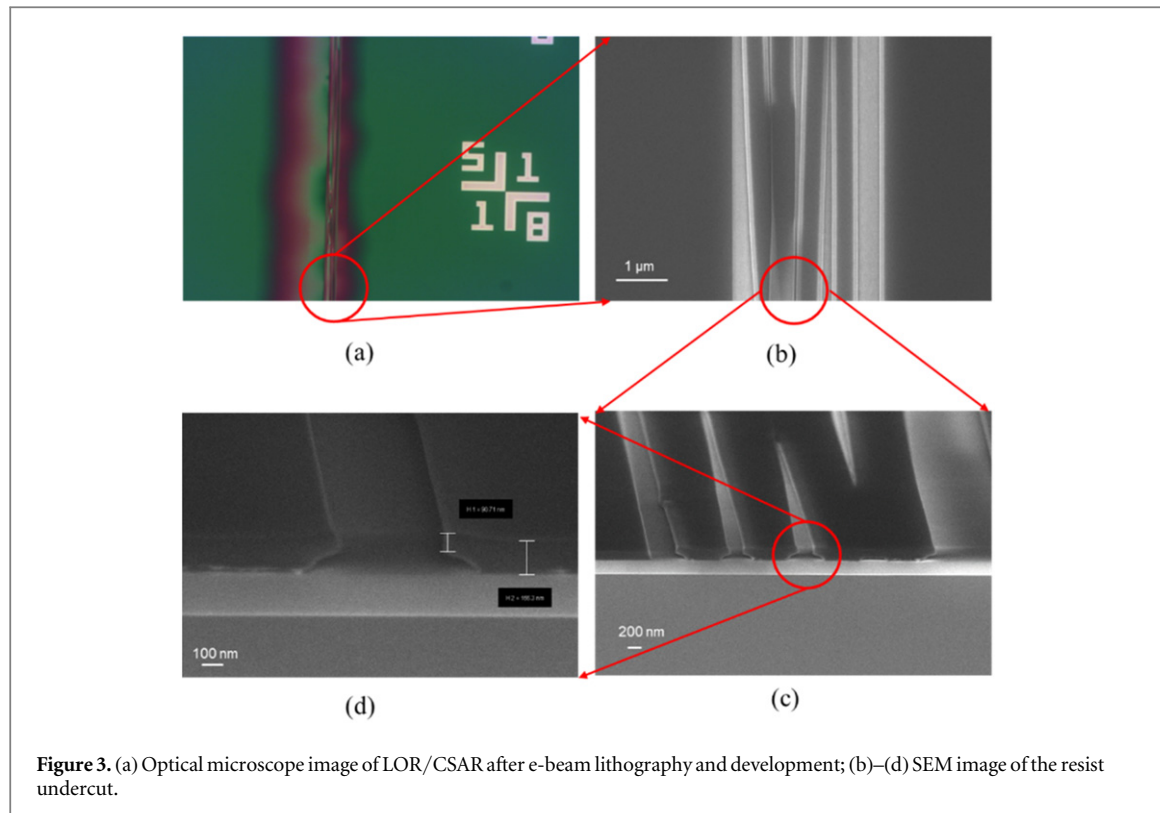


Figure 3. (a) Optical microscope image of LOR/CSAR after e-beam lithography and development; (b)–(d) SEM image of the resist undercut.

3.2. Height characteristic analysis

Skewness (R_{sk}) and Kurtosis (R_{ku}) are the height characteristic average parameters of a surface. Skewness is the third central moment of profile amplitude probability density function, measured over sample length. Skewness is a measure of the asymmetry of the profile about the mean line. Negative skew indicates a predominance of valleys, while positive skew is seen on surfaces with peaks. Kurtosis the fourth central moment of profile amplitude probability density function, measured oversampling length. Skewness is a measure of the distribution of spikes above and below the mean line. The mathematical definition of Skewness (R_{sk}) and Kurtosis (R_{ku}) follows:

$$R_{sk} = \frac{1}{R_q^3} \left(\frac{1}{l} \int_0^l Z^3(X) dx \right) \quad (3)$$

$$R_{ku} = \frac{1}{R_q^4} \left(\frac{1}{l} \int_0^l Z^4(X) dx \right) \quad (4)$$

where R_q is the root mean square (RMS) average between the height deviations and the mean line/surface, taken over the evaluation length/area. Z is the amplitude of each point of the measured length l . Figure 4 schematically depicts the surface profile with different skewness and kurtosis. The surface roughness parameters and height characteristic parameters of samples A, B, and C before and after dry etching and HF treatment are shown in table 1. AFM height image of samples is shown in figure 5.

The roughness average (R_a) and root mean square roughness (R_{rms}) are found to be 0.81 nm and 1.02 nm before and after dry etching respectively. This indicates that the dry etching is not affecting the SiO_2 that much. On the other hand after HF treatment the values reduced to 50% of original values. The skewness and kurtosis vary very little after dry etching indicating that the surface is almost unchanged, whereas the skewness changes from negative to positive after HF treatment. A negative skewness indicates that a greater percentage of the profile is above the mean line and a positive value indicates that a greater percentage is below the mean line. Kurtosis values increased almost 6 times after HF treatment. For, R_{ku} values greater than 3 represents spiky surfaces and R_{ku} values less than 3 represents the bumpy surface. Figure 5 shows the AFM height images of the samples A, B and C. From the height distribution data and height distribution profile it's evident that the partial SiO_2 etching increases the roughness of the surface which negatively effects the adhesion some liquids to the surface.

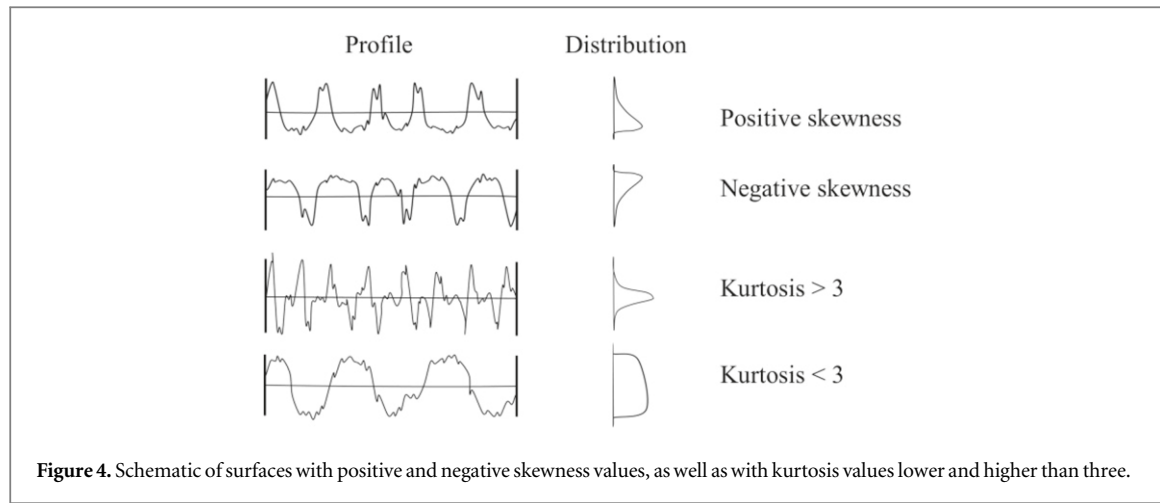
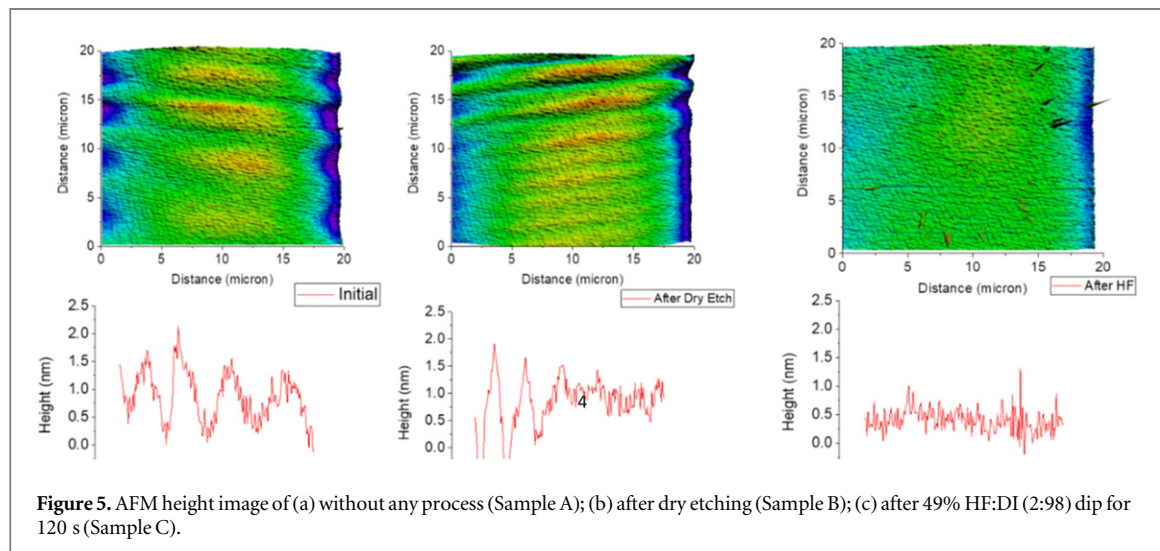


Table 1. Different surface texture parameters acquired by AFM.

Parameter	Initial	After dry etch	After HF treatment
R_a	0.81 nm	0.81 nm	0.42 nm
R_{rms}	1.02 nm	1.01 nm	0.56 nm
R_{max}	17.47 nm	6.86 nm	12.57 nm
R_{sk}	-0.828	-0.948	0.471
R_{ku}	4.448	3.635	17.189



4. Surface characterization using contact angle

It has been shown that the surface properties changed greatly after dry etching and HF treatment while remained almost unchanged after dry etching alone. Thus, HF treatment may be the main reason leading to the adhesion problem. In order to evaluate the surface adhesion changes associated with surface properties due to HF treatment, contact angle measurements are conducted in this paper. Contact angle, by definition, is the angle formed between the droplet of liquid and solid surface and is one of the most common ways to characterize the adhesion between solid surface and liquid. Specifically, a small contact angle means good adhesion while large angle means poor adhesion [15]. One of the contact angle measure methods, a direct optical measurement based on Telescope-Goniometer method, is used to obtain the static contact angle of each sample. The volume of droplet is controlled around 15 μ l for consistency and accurate trend.

Figures 6(a) and (b) show the contact angle measurement results for LOR resist on SiO_2/Si substrate without any treatment and after HF treatment. It can be clearly seen that the contact angle increases from 29.26 degrees

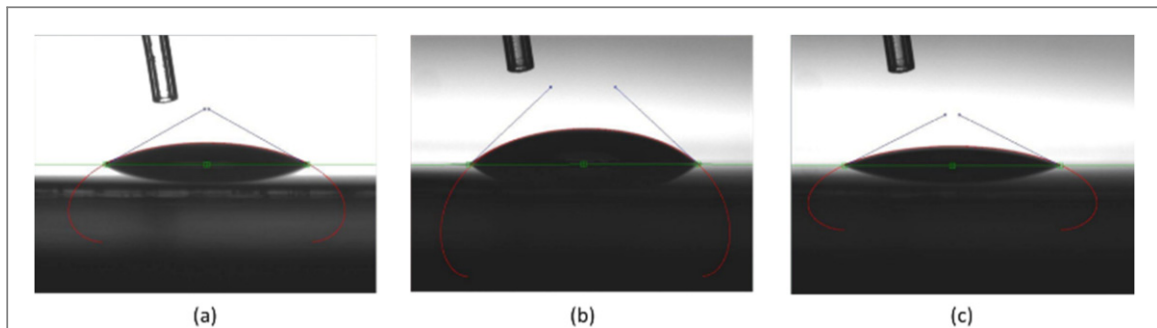


Figure 6. Contact angle measurement of LOR (PMGI) resist on SiO_2/Si substrate (a) Before any treatment with angle 29.26 degrees; (b) After HF treatment with contact angle 43.24 degrees; (c) After HMDS application with contact angle 26.76 degrees.

to 43.24 degrees, indicating the surface adhesion became poorer after HF treatment. This result agrees with AFM results and suggests that HF treatment indeed cause adhesion problem between

LOR resist and SiO_2/Si substrate. This problem can be addressed by applying HMDS promoter [16], which is confirmed by the decrease in contact angle (figure 6(c)).

The contact angle is usually characterized by Young's equation, which shows the balance among three media (vapor, liquid and solid):

$$\gamma_s = \gamma_l \cos \theta + \gamma_{sl} \quad (5)$$

where γ_s is the surface free energy (SFE) of the solid surface, γ_{sl} is the SFE of the interface between solid and liquid droplet, γ_l is the SFE of the liquid droplet, and θ is the contact angle [15, 17]. SFE can usually be divided into two independent parts: dispersion part (γ^d) and polar part (γ^p) representing interactions due to dispersion components and polar components, as shown in equations (6) and (7):

$$\gamma_s = \gamma_s^d + \gamma_s^p \quad (6)$$

$$\gamma_l = \gamma_l^d + \gamma_l^p \quad (7)$$

Owens and Wendt determined the SFE of the interface between solid and liquid (γ_{sl}) as follows [17, 18]:

$$\gamma_{sl} = \gamma_s + \gamma_l - 2(\gamma_s^d \gamma_l^d)^{0.5} - 2(\gamma_s^p \gamma_l^p)^{0.5} \quad (8)$$

where the sum of third and fourth terms can be defined as the adhesion energy between solid surface and liquid [18]:

$$W_A = 2(\gamma_s^d \gamma_l^d)^{0.5} + 2(\gamma_s^p \gamma_l^p)^{0.5} \quad (9)$$

From equations (5)–(9), the γ_s^d and γ_s^p can be determined by contact angle measurement results from two liquids with known γ_l^d and γ_l^p . Therefore, we conducted the following experiments. SiO_2/Si substrate surfaces before and after HF treatment are characterized by water and diiodomethane (CH_2I_2). Water and diiodomethane are well known liquids on opposite ends of the polarity spectrum where water is predominantly polar ($\gamma_l^d = 21.8 \text{ mJ m}^{-2}$ and $\gamma_l^p = 51 \text{ mJ m}^{-2}$) and diiodomethane has no polar component ($\gamma_l = \gamma_l^d = 50.8 \text{ mJ m}^{-2}$) [17, 18].

Use of these two liquids allows for the Owens-Wendt model to be applied directly in this study. Figure 7 shows the contact angle measurements for water and diiodomethane on SiO_2/Si substrate before and after HF treatment. From the measured contact angle and SFE of water and diiodomethane,

SFE (both dispersive and polar parts) of SiO_2/Si substrate surfaces and adhesion energy (between diiodomethane and SiO_2/Si substrate) before and after HF treatment can be calculated, as shown in table 2. The dispersion part of the SiO_2/Si substrate after HF treatment actually decreased from 39.71 mJ m^{-2} to 36.82 mJ m^{-2} and the polar part increased from 28.88 mJ m^{-2} to 37.67 mJ m^{-2} . As a result, the adhesion energy between diiodomethane and SiO_2/Si substrate decreased from 89.83 mJ m^{-2} to 86.5 mJ m^{-2} , indicating poorer adhesion after HF treatment. It is well known that LOR resist also has a dominant dispersion part like diiodomethane, thus the adhesion energy between LOR resist and SiO_2/Si substrate surfaces will also decrease after HF treatment, leading to the aforementioned adhesion problem. On the other hand, PMMA has a relatively smaller dispersion part ($\gamma_l^d = 29.6 \text{ mJ m}^{-2}$ and $\gamma_l^p = 11.5 \text{ mJ m}^{-2}$) [19], thus preventing the surface adhesion problem for the samples after HF treatment.

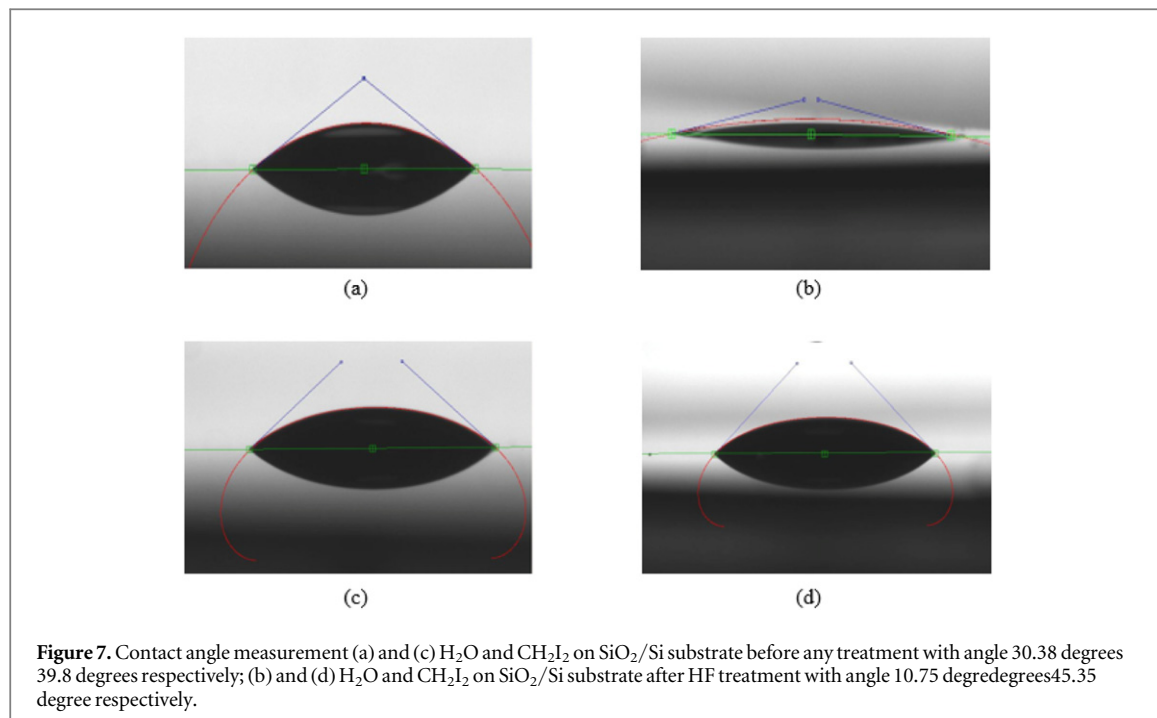


Figure 7. Contact angle measurement (a) and (c) H_2O and CH_2I_2 on SiO_2/Si substrate before any treatment with angle 30.38 degrees 39.8 degrees respectively; (b) and (d) H_2O and CH_2I_2 on SiO_2/Si substrate after HF treatment with angle 10.75 degrees 45.35 degree respectively.

Table 2. Different surface energy components acquired by contact angle measurements.

Parameter (Units: mJ m^{-2})	Before HF treatment	After HF treatment
Dispersion part of SiO_2/Si substrate (γ_s^d)	39.71	36.82
Polar part of SiO_2/Si substrate (γ_s^p)	28.88	37.67
Adhesion energy between SiO_2/Si substrate and CH_2I_2 (W_A)	89.83	86.50

5. Summary

Wet etching i.e. Hydrofluoric acid etching significantly alters the surface morphology of SiO_2 . The wet etching of SiO_2 increases the roughness of the surface by modifying the third and fourth moments of the density function namely skewness and kurtosis. HF wet etching turns the negative skewness height distribution profile to positive skewness and increases the kurtosis far greater than 3. These changes in morphology decrease surface adhesion by reducing the real contact area of the surface, leading to an increased contact angle. Dry etching almost does not change the SiO_2 morphology at all. For sensitive fabrication processes where it is necessary to etch SiO_2 partially, it is recommended to use dry etching instead of HF wet etching. In the cases where HF wet etching is inevitable, it is recommended to use surface promoter such as HMDS to preserve the surface adhesion. Alternatively, other another type of resist such as PMMA (where the dispersion component is less dominant in the surface free energy) can be an option to avoid adhesion problem.

ORCID iDs

Kazy F Shariar  <https://orcid.org/0000-0002-3018-3907>

References

- [1] Kim S-K, Jung M-H, Kim H-W, Woo S-G and Lee H 2005 *Nanotech.* **16** 2227–32
- [2] Bauer J, Drescher G and Illig M 1996 *J. Vac. Sci. Technol. B* **14** 2485
- [3] Dammel R 1993 Diazonaphthoquinone-based resists *TT 11, Tutorial Text in Optical Engineering* (Bellingham, WA: SPIE—The International Society for Optical Engineering)

- [4] Deckert C A and Peters D A 1983 Adhesion, Wettability, and Surface Chemistry *Adhesion Aspects of Polymeric Coatings* ed K L Mittal (Boston, MA: Springer) pp 469–98
- [5] Tanaka T, Morigami M, Oizumi H, Ogawa T and Uchino S 1994 *Japan J. Appl. Phys.* **33** 1803
- [6] Hoshino T and Nishioka Y 1999 *Journal of Chemical Physics* **111** 2109
- [7] Takahagi T, Nagai I, Ishitani A and Kuroda H 1988 *Journal of Applied Physics* **64** 3516–21
- [8] Higashi G S, Chabal Y J, Trucks G W and Raghavachari K 1990 *Appl. Phys. Lett.* **56** 656
- [9] Tanaka T, Morigami M and Atoda N 1993 *J. Electrochem. Soc.* **140** L115
- [10] Jincao Y and Matthews M 2001 *Ind. Eng. Chem. Res.* **40** 5858
- [11] Kim S K 2003 *J. Korean Phys. Soc.* **42** S371
- [12] Lee H J, Park J T, Yoo J Y, An I and Oh H K 2003 *J. Korean Phys. Soc.* **42** S202
- [13] Kawai A and Inoue D 2002 *Journal of Photopolymer Science and Technology* **15** 5757–8
- [14] Mehta S S, Qin S H, Mukherjee-Roy M, Singh N and Kumar R 2004 *Microelectronics Journal* **35** 427–9
- [15] Yuan Y and Lee T R 2013 Contact Angle and Wetting Properties *Surface Science Techniques (Springer Series in Surface Sciences)* ed G Bracco and B Holst vol 51 (Berlin: Springer) pp 3–34
- [16] https://microchemicals.com/technical_information/substrate_cleaning_adhesion_photoresist.pdf
- [17] Tomicic D 2002 *Adhesion measurements of positive photoresist on sputtered aluminium surface* DissertationInstitutionen för teknik och naturvetenskap
- [18] Zenkiewicz M 2007 *JAMME* **24** 137–45
- [19] <http://surface-tension.de/solid-surface-energy.htm>